JOURNAL OF AIRCRAFT
Vol. 33, No. 1, January–February 1996

Control of Pressure Oscillations in Deep Cavities Excited by Grazing Flow

Stephen F. McGrath* and David J. Olinger†
Worcester Polytechnic Institute, Worcester, Massachusetts 01609

Grazing flow over a deep cavity can result in acoustic resonance characterized by a standing wave–vortex feedback loop. Control of cavity resonance has potential impact in stealth aircraft and aircraft weapons bay applications, where periodic stress loading can cause material fatigue failure or damage sensitive instrumentation. A previous perturbation analysis of the fundamental equations of motion for a fluid system motivates a control method based on interaction of an external source of momentum (force) with cavity velocity fluctuations. Through proper placement of stationary control screens (force addition) within the resonant cavity in laboratory experiments, the cavity rms pressure amplitude was significantly reduced without interfering with the approaching boundary layer. Reductions in cavity base spectral peaks of up to 26 dB were achieved. Both single vortex (one-quarter mode shape) and double vortex (three-quarter mode shape) cases were controlled. Placement of control screens at locations of maximum velocity fluctuation yields optimum control for force addition.

Nomenclature

a = speed of sound
D = cavity depth
D_0 = added effective cavity depth
$\boldsymbol{D}'$ = fluctuating drag force on fluid
d = control screen depth
E = disturbance energy
e = internal energy (per unit mass)
$\boldsymbol{F}$ = external force vector
$\boldsymbol{F}'$ = fluctuating resultant force on fluid
f = frequency
f_n = nth harmonic frequency
L = cavity width
$\boldsymbol{L}'$ = fluctuating lift force on fluid
$\dot{m}$ = mass flow rate (per unit volume)
$P(f)$ = spectral density function
p = pressure
$\dot{Q}$ = heat transfer rate
$\boldsymbol{q}$ = heat flux vector
$\boldsymbol{q}'$ = fluctuating heat flux
St = Strouhal number, (f_nL/U_∞)
s = entropy (per unit mass)
T = temperature
T_0 = fluid temperature at reference state
U_∞ = freestream velocity
$\boldsymbol{v}$ = velocity
$\boldsymbol{v}'$ = fluctuating velocity
x = cavity width coordinate
y = cavity depth coordinate
θ = angle between fluctuating force and fluctuating velocity vectors
ρ_0 = fluid density at reference state
σ = energy source (control) term
σ_c = cavity base rms pressure amplitude (control)
σ_c/σ_0 = normalized cavity base rms pressure
σ_0 = cavity base rms pressure amplitude (no control)
$\bar{\bar{\tau}}$ = viscous stress tensor
Φ = energy dissipation term

Presented as Paper 94-2220 at the AIAA 25th Fluid Dynamics, Plasmadynamics, and Lasers Conference, Colorado Springs, CO, June 20–23, 1994; received July 17, 1994; revision received June 23, 1995; accepted for publication June 26, 1995.

*Graduate Student, Mechanical Engineering Department; currently at Wright Laboratory, Wright–Patterson AFB, OH 45433.
†Assistant Professor, Mechanical Engineering Department. Member AIAA.

Introduction

FLOW across a sharp-edged deep cavity can induce acoustic resonance. A good illustration of this effect is the tone produced by blowing across a bottle opening. If intense enough this cavity resonance can, over time, cause structural fatigue failure due to periodic stress loading from the acoustic oscillations.[1] Control of the resonance has application in aircraft wheel well and weapons bays, piping systems, and valves. Stealth technology, which depends in part on storing ordinance within cavity structures until deployment, is also affected by this resonance condition. Sensitive instrumentation can also be damaged by intense pressure oscillations in a weapons bay.[2]

Extensive reviews of the dynamics of unstable flows past cavities are found in Rockwell and Naudascher[1] and Komerath et al.[3] Two types of cavities that sustain resonant conditions have generally been studied. Shallow cavities, which have an AR of $L/D >> 1$, are characterized by longitudinal modes.[3] Deep cavities ($L/D << 1$) are characterized by a standing wave–vortex interaction and acoustic depth modes (Fig. 1). In resonant cavities, the shear layer separating the exterior flow from the cavity flow is naturally unstable. This instability excites normal cavity standing wave modes in deep cavities. The resultant oscillations in the cavity strengthen the shear-layer instability and a feedback loop is initiated.[1,3] The precise mechanism that sustains this feedback loop has been the subject of numerous studies over the past 30 years and is still an open question.

Erickson and Durgin[4,5] studied the mechanism sustaining the feedback loop in a deep cavity (Fig. 1). They found that vortex formation and subsequent impingement on the cavity trailing edge at the resonant condition was a key to the feedback loop. The resonance frequency for a square, deep cavity is given by

$$f_n = [(2n - 1)/4][a/(D + D_0)] \qquad n = 1, 2, \ldots \quad (1)$$

$$St = f_nL/U_\infty \quad (2)$$

where D_0 accounts for end effects that tend to lower the resonance frequency. Erickson and Durgin proposed that when

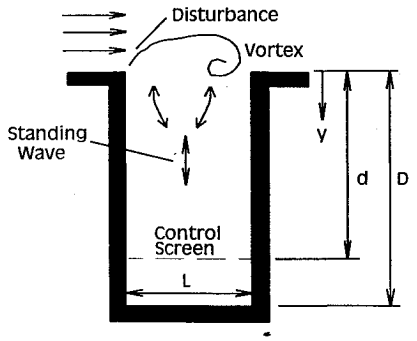

Fig. 1 Resonant cavity geometry.

a cavity resonates, the standing wave–vortex feedback loop is initiated, and a lock-on condition results. Along with Rockwell and Naudascher[1] they found that the feedback loop was primarily wave driven for deep cavities.

Graf and Durgin[6,7] used laser Doppler velocimetry to study the flow field dynamics in a cavity at resonance. The Strouhal numbers for deep cavity resonance in Eq. (2) were determined experimentally. At the freestream velocity corresponding to resonance at the fundamental cavity frequency $St \approx 0.3$ a single vortex (SV) mode was observed. This mode is characterized by a single vortex resident in the cavity opening at any time. At the freestream velocity corresponding to the first odd harmonic of the cavity $St \approx 0.8$, a double vortex (DV) mode with two resident vortices was observed.

Gharib and Roshko[8] studied the effects of varying AR on the self-sustaining oscillations in an axisymmetric cavity. For cavities with normalized lengths below a value of 80, the shear layer bridges the entire cavity opening and no resonance occurs. Two other modes, modes II and III, corresponded to either two or three vortical structures in the cavity during resonance, respectively. The mode II region marked the onset of self-sustaining oscillations for the cavity. Between the mode II and III regions, Gharib and Roshko found a distinct transition (hysteresis) region. The role of the mean momentum transfer and Reynolds stress in the shear layer on cavity drag was also investigated.

Various methods of resonance control have been attempted in deep cavities. Rockwell and Naudascher[1] and Komerath et al.[3] review attenuation of cavity oscillations concentrating on geometric alterations (ramps, spoilers) for resonance control. Examples of mass injection at the leading-edge lip of a cavity, leading to considerable control of the periodic oscillations, are also cited.

Coffman and Bernstein[9] studied the problem of resonance in gas pipeline valves with deep cavity geometries. The only effective form of resonance control found for the valves was geometric redesign of the valve cavities. Eisinger[10] investigated the suppression of standing waves in tube heat exchangers and determined that baffles, placed parallel with the freestream flow and perpendicular to the standing waves, resulted in considerable control of the cavity oscillations.

Control studies on grazing flow past resonant cavities generally have utilized significant geometry change or addition of a device that modifies the approaching boundary-shear layer. Geometric redesign may be expensive or impractical to perform on aircraft structures and shear-layer intrusive control techniques can increase drag levels. In the current study the perturbation analysis developed by Chu,[11] and further studied by Raghu and Sreenivasan,[12,13] is used to motivate new control techniques using control screens to extract energy from the resonant standing wave in deep cavities.

In the next section the perturbation analysis of Chu and Raghu and Sreenivasan is reviewed and the general features of the present control methods are discussed. The experimental procedures used to apply these control methods in a laboratory cavity flow are then described. Results are presented for both the single and double vortex mode cases. Finally, implications of the present study and future directions are detailed.

Perturbation Analysis

A previous analysis by Chu[11] motivates the control techniques used in the present study. Chu analyzed the growth of perturbations in resonant fluid flow systems. Through an analysis of the fundamental mass, momentum, and energy equations, Chu (and later Raghu[12] and Raghu and Sreenivasan[13]) determined that a single term in a conglomerate mass, momentum, and energy equation governs how energy can be extracted from an unstable system. The fundamental equations of motion

$$\frac{d\rho}{dt} + \rho(\nabla\cdot v) = \dot{m} \quad \text{(conservation of mass)} \tag{3}$$

$$\rho\frac{dv}{dt} + \nabla p = \nabla\cdot\bar{\bar{\tau}} + F \quad \text{(momentum)} \tag{4}$$

$$\rho\left[\frac{de}{dt} + p\frac{d(1/\rho)}{dt}\right] = (\bar{\bar{\tau}}:\nabla v) - (\nabla\cdot q) + \dot{Q} \quad \text{(energy)} \tag{5}$$

are used as a starting point. Here, $\dot{m}$, F, and $\dot{Q}$ are external sources of mass, force, and heat transfer, respectively.

Chu performed a perturbation analysis [Eqs. (6–8)] of these equations

$$\frac{\partial\rho'}{\partial t} + \rho_0(\nabla\cdot v') = \dot{m}' \tag{6}$$

$$\rho_0\frac{\partial v'}{\partial t} + \nabla p' = (\nabla\cdot\bar{\bar{\tau}}') + F' \tag{7}$$

$$\rho_0\frac{\partial s'}{\partial t} + \left(\nabla\cdot\frac{q'}{T}\right) = \frac{\dot{Q}'}{T_0} \tag{8}$$

The primed terms denote the fluctuating components and the energy equation has been rewritten in terms of an entropy balance.[11] An energy balance for a fluid flow system [Eqs. (9–12)] is then developed:

$$\frac{\partial E}{\partial t} + (\nabla\cdot J) = -\Phi + \sigma \tag{9}$$

where

$$J = p'v' - (\bar{\bar{\tau}}'\cdot v') + (T'q'/T_0) \tag{10}$$

$$\Phi = (\bar{\bar{\tau}}':\nabla v') - (1/T_0)(q'\cdot\nabla T') \tag{11}$$

$$\sigma = F'\cdot v' + \dot{m}(p'/\rho_0) + T'(\dot{Q}'/T_0) \tag{12}$$

Here, $\nabla\cdot J$ is a diffusion term, Φ represents viscous dissipation, and the σ represents the energy addition to a fluid system through the interaction of external sources of mass, momentum, and energy with fluctuation quantities. E is a nonnegative quantity, which vanishes only when fluctuations are not present[11]:

$$E = \rho_0 v'\cdot\frac{\partial v'}{\partial t} + \frac{p'}{\rho_0}\frac{\partial\rho'}{\partial t} + \rho_0 T'\frac{\partial s'}{\partial t} \tag{13}$$

Integrating Eq. (9) over a closed region R, Chu developed an equation representing the energy interactions in the fluid medium:

$$\frac{\partial}{\partial t}\int_R E(d^3x) + \int_{CS} J\cdot dA = -\int_R \Phi(d^3x) + \int_R \sigma(d^3x) \tag{14}$$

The first term on the left in Eq. (14) represents the disturbance energy gained by a fluid system over a cycle of time, while the second term is the energy radiated from the control surface by diffusion. The first term on the right of Eq. (14) is the energy dissipation term, which is related to the entropy production per unit mass $\dot{s}$ and is always positive.

Inspection of the last term in Eq. (14), along with Eq. (12), reveals three source/fluctuation pairs[11]: 1) force sources coupled with velocity fluctuations, 2) mass sources coupled with pressure fluctuations, and 3) heat sources coupled with temperature fluctuations. Correct addition of these source terms in the proper phase with the fluctuations will lead to suppression of the resonant condition. Chu's analysis also included multiple chemical species and the effect of molar concentration fluctuations on energy interactions. These are not included here for simplicity.

The current study concentrates on suppression of the cavity resonance through force addition to the system. From Eqs. (12) and (14), we can isolate the momentum term:

$$\int_R \frac{\partial E}{\partial t}\, d^3\boldsymbol{x} = \int_{CV} (\boldsymbol{F}' \cdot \boldsymbol{v}')\, d^3\boldsymbol{x} \qquad (15)$$

The left-hand term in Eq. (15) represents the change in disturbance energy within a fluid control volume. For the right-hand integral, the $\boldsymbol{F}'$ term represents a source of force addition, while the $\boldsymbol{v}'$ term represents the fluctuating component of velocity. If the integral on the right-hand side (RHS) of Eq. (15) is negative, energy is extracted, and the disturbance is suppressed. The sign of the integral is dependent on the geometric orientation (dot product) between the resultant force on the fluid and the velocity fluctuations.

It can be shown[14,15] that a screen placed perpendicular to $\boldsymbol{v}'$ in a cavity will create a resultant force $\boldsymbol{F}'$ on the fluid that is oriented between 90–270 deg from the velocity fluctuations (Fig. 2). For such a screen positioning, the integral on the RHS of Eq. (15) will always be negative, leading to energy extraction. Also, larger $|\boldsymbol{v}'|$ fluctuation levels should generally lead to more effective control, since the resultant force fluctuations vary approximately as $\boldsymbol{F}' \propto |\boldsymbol{v}'|^2$ in the nonlinear regime. The threshold for nonlinearity depends on the screen diameter used. The resultant force is also related to the screen cylinder diameter and length (i.e., solidity). The limiting case of a solid screen would change the resonant frequency of the cavity, and therefore, is not useful for controlling resonance.

Raghu[12] and Raghu and Sreenivasan[13] applied these control methods to an impressive array of resonant fluid systems, including Rijke tubes, whistler nozzles, organ–pipe resonators, and a combustion wind tunnel. Techniques involving force addition (using control screens), mass addition, and heat addition from Eq. (12) were used. Both passive and active feedback control methods were studied. Significant suppression of the resonant oscillations was demonstrated. The current study extends these control methods to grazing flow over resonant cavities.

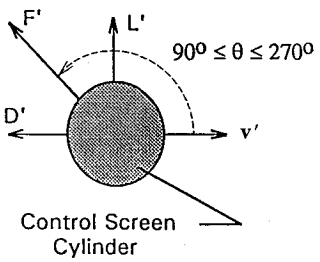

Fig. 2 Interaction of fluctuating force and velocity vectors.

Experimental Methods

All of the experiments were conducted in the Worcester Polytechnic Institute Thermal and Fluids Processes Laboratory in a single contraction subsonic wind tunnel with a 45.7 × 61.0 cm test section of 91.4 cm length. A square (L = 6.35 cm) Plexiglas® sharp-edged deep cavity was constructed with the flanged cavity sections depicted in Fig. 3. Four separate square cavity sections, with varying depth dimensions, were used so that control screens could be placed at several d/D positions (see Fig. 3). The depth of the various sections ranged from 4.85 to 8.50 cm. An adjustable cavity bottom allowed for varying cavity AR ($0.139 \leq L/D \leq 0.254$).

The two resonance conditions identified by Graf and Durgin[6,7] were studied: single vortex, fundamental frequency (SV), and double vortex, first odd harmonic (DV). Schematics of the pressure and velocity mode shapes for the two resonant cases are depicted in Fig. 4. For excitation of the fundamental frequency, mode shapes approximated a quarter sine wave shape;

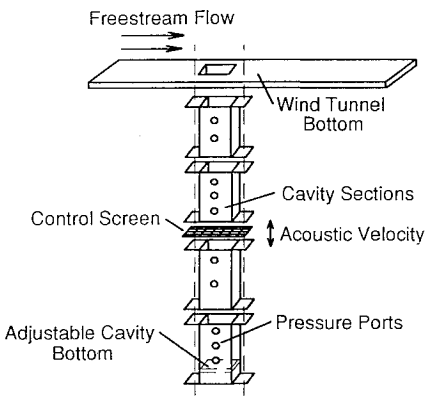

Fig. 3 Experimental apparatus (not to scale).

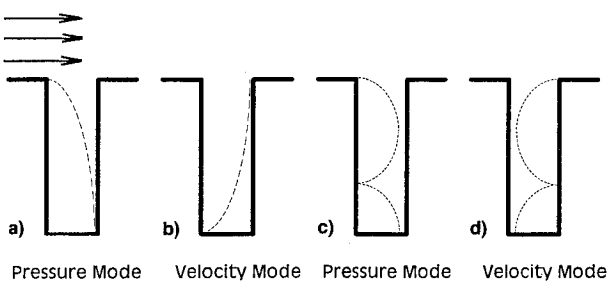

Fig. 4 Pressure and velocity mode shapes: a) and b) fundamental frequency (single vortex mode, St = 0.3) and c) and d) first odd harmonic (double vortex mode, St = 0.8). Zero reference at cavity leading-edge lip.

Table 1 Experimental conditions for single and double vortex modes

Vortex	St	D, cm	L/D	f_n [Eq. (1)], D_0 = 0, Hz	f_n, exp, Hz	U_∞, m/s
Single	0.304	25	0.254	346	≈315	65.7
Double	0.745	38	0.167	683	≈645	55.0

for the first odd harmonic, a three-quarters sine wave was observed. Table 1 summarizes the experimental conditions for cavity resonance for the cases examined in the present study. Since the added effective length in Eq. (1), D_0, is not known a priori, we present the predicted resonance frequency with $D_0 = 0$. Comparison of the measured and predicted resonance frequencies yields an average $D_0 = 0.08D$ for the two modes.

For the single vortex mode d/D values of 0.0, 0.024, 0.222, 0.469, and 0.948 were studied. Control screen percent open area varied from 30 to 70%. For the double vortex mode d/D values of 0.0, 0.015, 0.145, 0.310, 0.67, 0.708, 0.86, and 0.974 were studied, with the control screen percent open area limited to the 30% case.

Table 2 Pressure port positions for the single and double vortex modes

Pressure port no.	y/D, SV	y/D, DV
1	0.076	0.050
2	0.172	0.113
3	0.300	0.197
4	0.400	0.263
5	0.568	0.374
6	0.756	0.497
7	0.956	0.629
8	—	0.753
9	—	0.853
10	—	0.963

Pressure measurements were taken using flush-mounted microphones from PCB Piezoelectronics, Inc. (model 106B) located on the cavity sidewall as shown in Fig. 3. These microphones have 300 mV/psi sensitivity with resolution of 10^{-4} psi rms. Table 2 shows the pressure port positions for the single and double vortex cases. A personal computer based data acquisition system with a National Instruments® AT-MIO-16F-5 data acquisition board and LABVIEW® software was used. Typical pressure records of one second length at sampling rates of 9000 and 20,000 Hz for the single and double vortex modes, respectively, were acquired. All Fourier spectra presented are averaged over at least three record lengths. Further details of the experimental apparatus can be found in Refs. 14 and 15.

Results

Single Vortex Mode

Figure 5 shows the effect of the optimum placement ($d/D = 0.024$) of a control screen on the resonant cavity pressure oscillations measured by the pressure transducer at $y/D = 0.956$. The no control (empty cavity) time trace and power spectrum are shown in Figs. 5a and 5b. Placement of the control screen (30% open area, $d/D = 0.024$) into the cavity results in suppression of the fundamental mode at 315 Hz with spectral peak reductions on the order of 26 dB (Figs. 5c and 5d). Spectral noise levels at low frequencies are reduced,

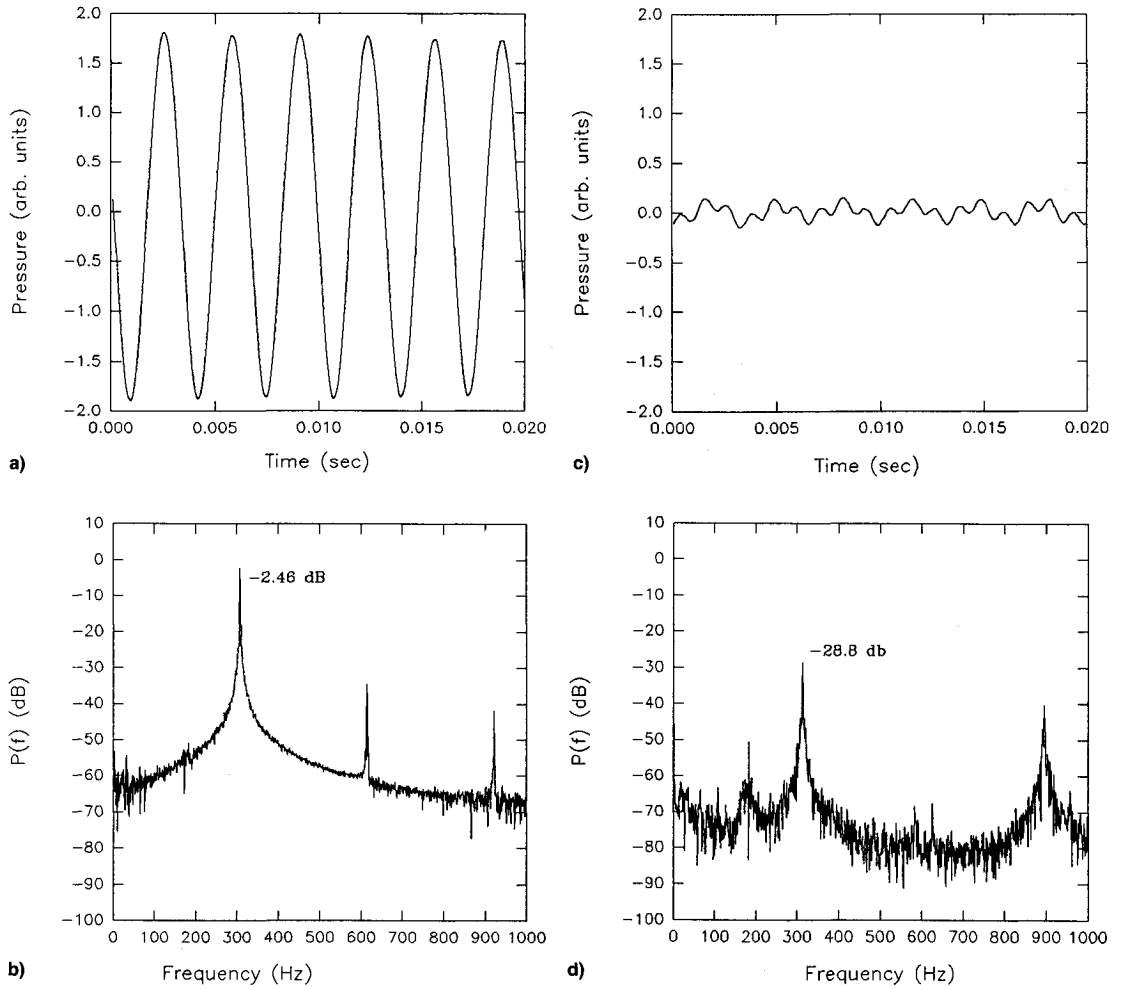

Fig. 5 Time traces and Fourier spectra for control of single vortex mode: a) and b) no control and c) and d) 30% open area control screen at $d/D = 0.024$. The parameters σ_0 and σ_c denote the rms pressure amplitude for the no control and controlled cases, respectively. $D = 25$ cm, $L/D = 0.254$, $U_\infty = 65.7$ m/s, pressure port at $y/D = 0.956$.

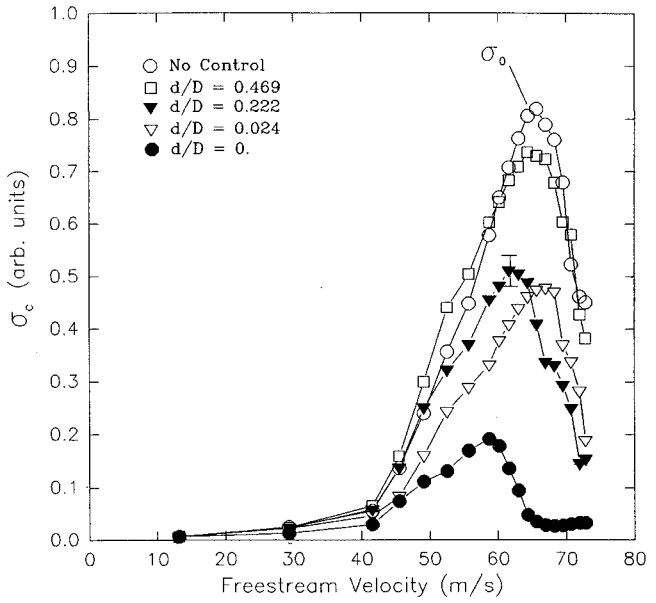

Fig. 6 Freestream lock-on velocity for various control screen positions, single vortex mode. D = 25 cm, L/D = 0.254, pressure port at y/D = 0.956, 57% open area control screen.

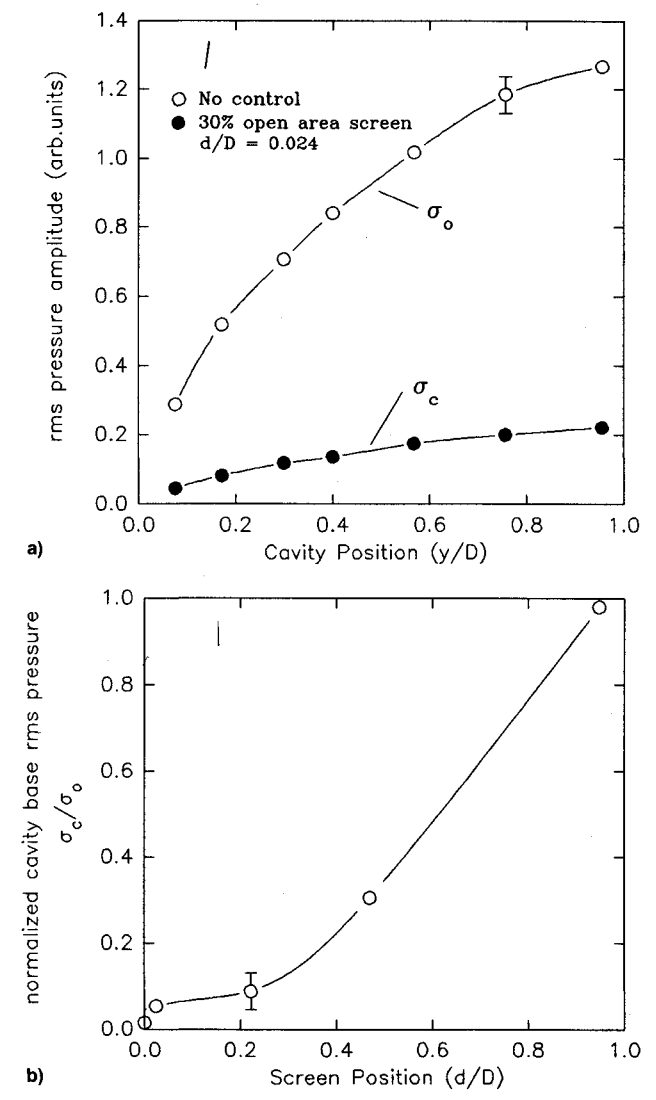

Fig. 7 a) Pressure mode shapes for the single vortex mode and b) effect of screen position on cavity base rms pressure amplitudes. D = 25 cm, U_∞ = 65.7 m/s, 30% open area screen.

revealing a peak at 180 Hz, which can be attributed to electrical sources. The reduction in spectral noise level is most probably due to viscous dissipation at small scales introduced by the control screen.

To determine if a shift in the cavity resonant frequency could occur due to the presence of the control screen, a freestream velocity variation was performed. Figure 6 shows the effect of varying the freestream velocity on the cavity base rms pressure level. Five cases were studied, including no control, and control screen placement at d/D = 0.0, 0.024, 0.222, and 0.469. The freestream lock-on velocity[5] for the no control case occurs at approximately 65 m/s where the cavity base rms pressure level reaches a maximum. No significant shift in the freestream lock-on velocity is observed as the control screen position is varied for a 57% open area screen. Reductions in the peak rms pressure levels for different d/D values are significantly larger than any reductions due to lock-on velocity shifts. Similar results were obtained for the least porous screen (30% open area). The limiting screen porosity required to cause a shift in resonance frequency was not determined in the current study.

The natural single vortex mode exhibits a quarter-mode shape resonance as shown in Fig. 7a, with minimum (maximum) rms pressure (velocity) levels at the cavity mouth. Figure 7a also presents the pressure mode shape for a controlled case (30% open area, d/D = 0.024), and shows that the local control technique results in a significant global suppression of the rms pressure amplitude.

Figure 7b shows the effect of control screen placement on the cavity base rms pressure levels. As discussed earlier, optimum control for this mode shape should occur with screen placement at the velocity fluctuation maxima near the cavity mouth and should decrease with deeper placement within the cavity. Our results confirm these trends. A sharp change in the cavity base pressure between the d/D = 0 and d/D = 0.024 is evident. This could indicate that two mechanisms for suppression are present. If the control screen is placed very near the cavity mouth, direct interference with shear layer formation may be occurring. However, we believe the control screen acts to extract energy from the resonant standing wave when placed deep in the cavity. Experimental results for the double vortex mode in the next section will further confirm this.

Screen percent open area, defined as the ratio of open area to cavity cross-sectional area L^2, was used to correlate the

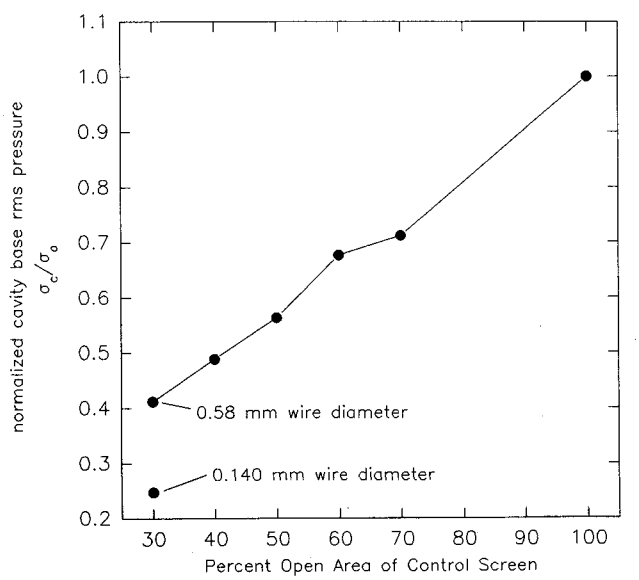

Fig. 8 Effect of control screen percent open area on cavity base rms pressure amplitudes, single vortex mode. D = 25 cm, U_∞ = 64.0 m/s, d/D = 0.024, pressure port at y/D = 0.956.

cavity base rms pressure level reductions. Figure 8 shows the effect of percent open area on cavity base rms pressure levels for a constant screen depth d/D. Cavity base rms pressure is reduced as the percent open area is decreased, with maximum control occurring at an open area of 30%, although lower percent open area screens were not tested. Caution should be taken when interpreting the results of Fig. 8, as another parameter, the screen wire diameter, was also found to affect the level of control. For example, two screens, both with 30% open area, but wire diameters varying by a factor of 4.2, were tested at the $d/D = 0.024$ control position. With the smaller diameter screen the cavity base rms pressure was found to be a factor of 1.66 lower than with the larger diameter screen.

It is postulated that the smaller diameter wire with its smaller pore size is more effective at damping small-scale fluctuations through the action of viscous dissipation [Φ term in Eq. (11)]. These results indicate that the level of control depends on both percent open area and the wire diameter, or fineness, of the control screen. The linearity of Fig. 8 can then be attributed to the similar relative fineness of the screens used in the study. Rice[16] and Hersh and Walker[17] have studied the flow resistance and acoustic impedance of fine screens in grazing flows.

Double Vortex Mode

The double vortex mode is of interest due to the three-quarter sine wave pressure mode shapes in the cavity (Fig. 9a). The resultant rms velocity levels are maximum where rms pressure levels are at a minimum. Figure 9a shows the anticipated optimum and ineffective positions for control screens using the earlier arguments. This mode shape should allow for effective control with screens placed deep within the cavity. Figure 9b shows the level of control (σ_c/σ_0) for various screen positions in the cavity.

It is evident that the most effective control of the pressure oscillations occurs near the mouth of the cavity and for $d/D \cong 0.667$. As expected, minimum control occurs for screen placement at the velocity nodes of $d/D = 0.310$ and $d/D = 1.00$. The level of control at $d/D = 0.66$ is significant, but approximately one-third of that for screen placement near the mouth of the cavity. This can be attributed in part to superposition of the fundamental (one-quarter) and first odd harmonic (three-quarters) mode shapes, since near the mouth of the cavity the velocity fluctuations are at a maximum for both modes, while deep in the cavity velocity fluctuations at the fundamental frequency fall to a minimum. Direct interference of the control screen with shear layer formation for small d/D may also play a role.

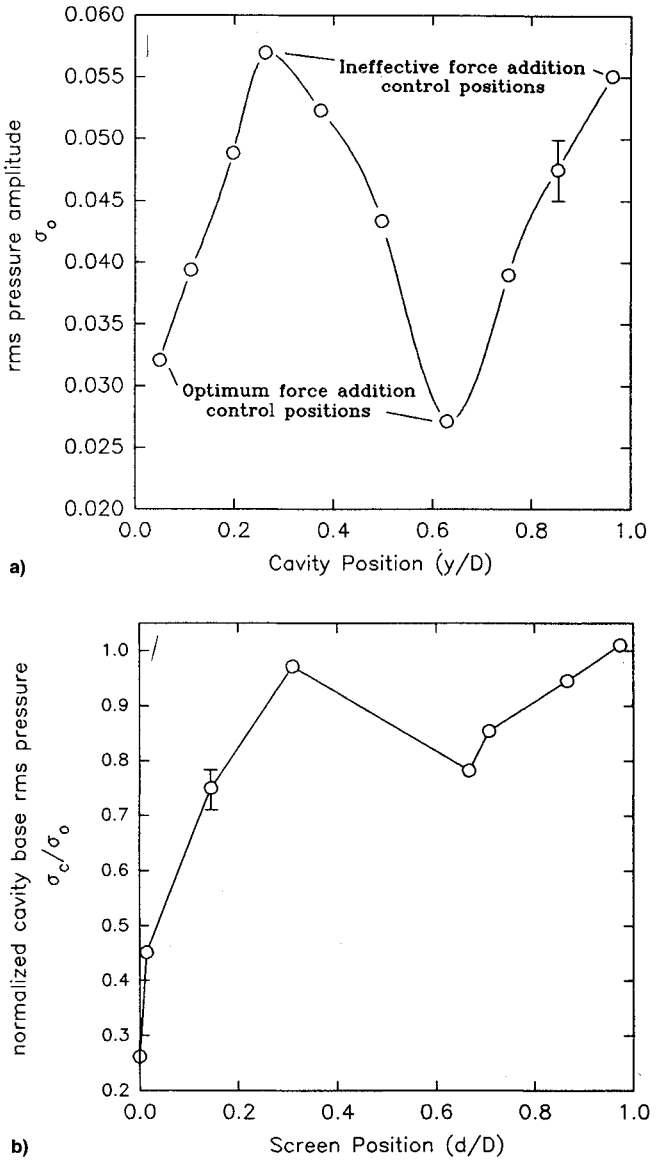

Fig. 9 a) Pressure mode shape for the double vortex mode, no control and b) effect of control screen position on cavity base rms pressure amplitudes. D = 38 cm, U_∞ = 55 m/s, 30% open area control screen.

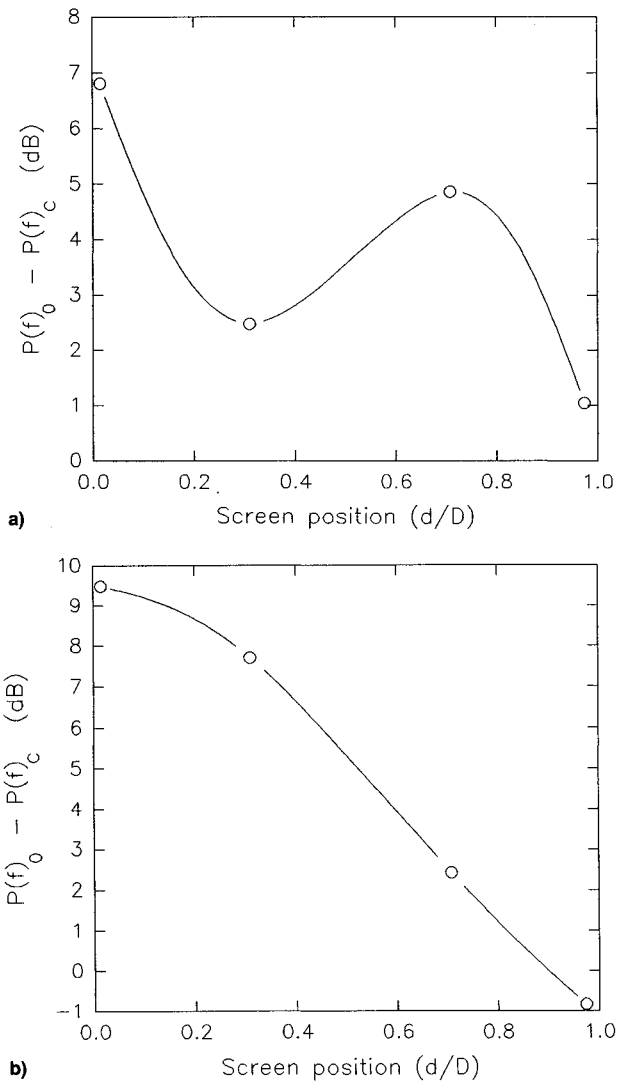

Fig. 10 Fourier spectral peak drop for the double vortex mode: a) first odd harmonic (645 Hz) and b) fundamental frequency (220 Hz). D = 38 cm, U_∞ = 55 m/s, pressure port at y/D = 0.963, 30% open area screen.

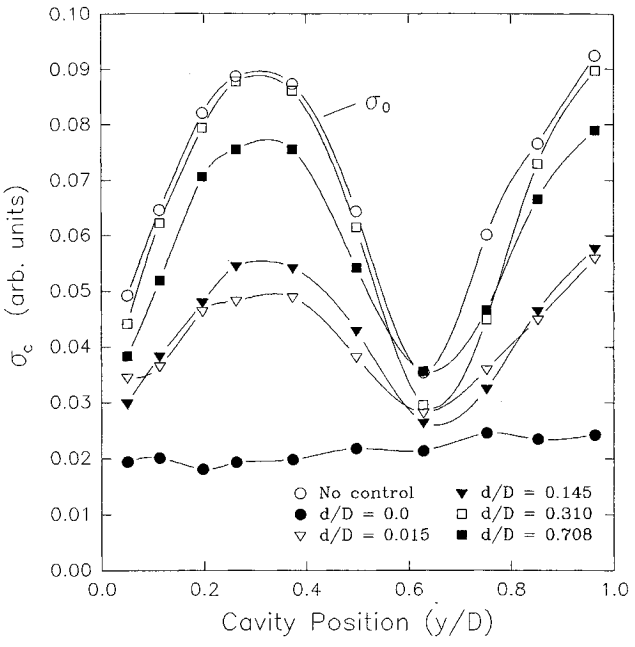

Fig. 11 Pressure mode shapes for the double vortex mode. D = 38 cm, U_∞ = 55 m/s, 30% open area control screen.

Figures 10a and 10b show the effect of control screen placement on the first odd harmonic and fundamental spectral peak levels. The curves resemble three-quarters and one-quarter sine wave shapes, similar to the velocity mode shapes for each respective mode in Figures 4b and 4d. These results indicate that the current control technique extracts energy in proportion to the relative amplitude of each mode.

Figure 11 shows pressure mode shapes (double vortex mode) for the natural case and five screen control positions. It is worthy to note that the $d/D = 0.310$ screen position offers better control in the $0.6D < y < 0.8D$ cavity depth range than the $d/D = 0.708$ screen position, even though the former is expected to be an ineffective position and the latter is an optimum placement. In this range Figs. 4a and 4c show that the effect of the fundamental frequency on the overall pressure mode shape is greater than that of the first odd harmonic. These results indicate that, even though the first odd harmonic may be the dominant frequency, the fundamental frequency still affects the control scheme.

Concluding Remarks

New control methods for deep cavities excited by grazing flow resulted in considerable suppression of cavity pressure oscillations. Sources of fluctuating force addition (control screens), in proper orientation with cavity velocity fluctuations, lead to energy extraction from the resonant system. Local control techniques lead to global suppression of rms pressure amplitudes throughout the resonant cavity with spectral peak reductions on the order of 26 dB.

Two cases for deep cavity resonance were examined, including single vortex, fundamental frequency excitation ($St = 0.3$), and double vortex, first odd harmonic excitation ($St = 0.8$). These conditions were of interest due to their respective one- and three-quarter sine wave mode shapes. Measurement of the mode shapes allowed for optimization of the control scheme for the two resonant conditions. Most effective control occurred for higher solidity screens placed at positions of maximum velocity fluctuations.

The control levels obtained (26-dB reductions in the dominant spectral peak) compare favorably with those found in previous deep cavity control studies such as Coffman[9] without introducing a significant geometry change or modifying the approaching boundary/shear layer. The present control methods and ideas may also offer insight into previous cavity resonance suppression, such as in Eisinger[10] and Rogers and Penterson,[18] who discuss placing baffles perpendicular to the resonant standing wave. Eisinger states that the baffles should be located in regions of maximum acoustic particle velocity for the particular wave that is to be eliminated. These baffles may operate using a similar mechanism as in the present study, although baffles can also create chambers with altered resonance frequencies within a cavity. Reinterpretation of previous control techniques in light of the increased fundamental understanding of suppression mechanisms gained in the current study may prove fruitful.

The question naturally arises whether the observed control is solely due to the action of the control term σ in Eq. (9). The effect of viscous dissipation [Φ term in Eq. (9)] has already been emphasized in the reduction in spectral noise levels (Fig. 5), and the increased effectiveness of small diameter control screens (Fig. 8). Chu[11] briefly introduced the possibility of manipulating the diffusion term in Eq. (9). Control screen placement at small d/D may also be manipulating shear-layer formation, thereby reducing the energy radiation by diffusion into the resonant cavity. However, for control screen placement deep within the cavity, the effect of the diffusion term can be considered small, since the characteristic mode shapes do not vary between the no control and control cases. As a result there is no shift in the phase relation between $p'$and v' necessary to significantly affect the diffusion term [Eq. (10)].

The generality of the perturbation analysis and control schemes suggests that extending the present ideas to shallow cavities characterized by resonant longitudinal modes will yield positive results. Use of force addition in a shallow cavity would entail placing control screens perpendicular to the freestream flow direction. Resonance control using passive fluctuating mass addition in proper phase with cavity pressure fluctuations [Eq. (12)] is also currently under study. Consistent with the present study, preliminary results show that placement of mass addition sources at rms pressure fluctuation maxima leads to the most effective control. We would also like to apply control ideas based on external sources of mass, momentum, and energy to open fluid flow systems such as resonant wake flows.

Acknowledgments

Support from a WPI Goddard Fellowship is acknowledged. The control methods developed by B. T. Chu, S. Raghu, and K. R. Sreenivasan are gratefully acknowledged. We thank S. Raghu and W. Durgin for useful discussions.

References

[1]Rockwell, D., and Naudascher, E., "Review—Self-Sustaining Oscillations of Flow Past Cavities," *Journal of Fluids Engineering*, Vol. 100, No. 2, 1978, pp. 152–165.

[2]Sarno, R. L., and Franke, M. E., "Suppression of Flow-Induced Pressure Oscillations in Cavities," *Journal of Aircraft*, Vol. 31, No. 1, 1994, pp. 90–96.

[3]Komerath, N. M., Ahuja, K. K., and Chambers, F. W., "Prediction and Measurement of Flows over Cavities—A Survey," AIAA Paper 87-0166, Jan. 1987.

[4]Erickson, D. D., and Durgin, W. W., "Tone Generation by Flow Past Deep Wall Cavities," AIAA Paper 87-0167, Jan. 1987.

[5]Erickson, D. D., "Unsteady Flow Past a Resonant Cavity: An Experimental Analysis of Flow-Induced Oscillations in a Deep Wall-Mounted Cavity," M.S. Thesis, Worcester Polytechnic Inst., Worcester, MA, 1987.

[6]Graf, H. R., and Durgin, W. W., "Measurement of the Nonsteady Flow Field in the Opening of a Resonating Cavity Excited by Grazing Flow," *Proceedings of the International Symposium on Nonsteady Fluid Dynamics*, Vol. 92, American Society of Mechanical Engineers, New York, 1990, pp. 409–416.

[7]Graf, H. R., and Durgin, W. W., "Flow Excited Acoustic Resonance: An Analytical Model," *Proceedings of the International Sym-*

posium on Flow-Induced Vibration and Noise, Vol. 7, American Society of Mechanical Engineers, New York, 1992, pp. 81–91.

[8]Gharib, M., and Roshko, A., "The Effect of Flow Oscillations on Cavity Drag," *Journal of Fluid Mechanics*, Vol. 177, No. 4, 1987, pp. 501–530.

[9]Coffman, J. T., and Bernstein, M. D., "Failure of Safety Valves due to Flow Induced Vibration," *Flow Induced Vibrations*, edited by S. S. Chen and M. D. Bernstein, Univ. Microfilms International, 1979, pp. 115–122.

[10]Eisinger, F. L., "Prevention and Cure of Flow-Induced Vibration Problems in Tubular Heat Exchangers," *Flow Induced Vibrations*, edited by S. S. Chen and M. D. Bernstein, Univ. Microfilms International, 1979, pp. 47–55.

[11]Chu, B. T., "On the Energy Transfer to Small Disturbances in a Fluid Flow: Part I," *Acta Mechanica*, Vol. 1, No. 3, 1965, pp. 215–234.

[12]Raghu, S., "Control of Combustion and Acoustically Coupled Fluid Dynamic Instabilities," Ph.D. Dissertation, Yale Univ., New Haven, CT, 1987.

[13]Raghu, S., and Sreenivasan, K. R., "Control of Acoustically Coupled Combustion and Fluid Dynamic Instabilities," AIAA Paper 87-2690, Oct. 1987.

[14]McGrath, S., and Olinger, D. J., "Suppression of Pressure Oscillations in Flow Past Resonant Cavities," AIAA Paper 94-2220, June 1994.

[15]McGrath, S. F., "Control of Pressure Oscillations in a Cavity Excited by Grazing Flow," M.S. Thesis, Worcester Polytechnic Inst., Worcester, MA, 1994.

[16]Rice, E. J., "A Model for the Acoustic Impedance of Linear Suppressor Materials Bonded on Perforated Plates," NASA TM82716, Oct. 1981.

[17]Hersh, A. S., and Walker, B., "Effects of Grazing Flow on the Steady-State Flow Resistance and Acoustic Impedance of Thin Porous-Faced Liners," NASA CR2951, Jan. 1978.

[18]Rogers, J. D., and Penterson, C. A., "Predicting Sonic Vibration in Cross-Flow Heat Exchangers—Experience and Model Testing," American Society of Mechanical Engineers Paper 77-WA/DE-28, Nov. 1977.